

Nonresonant excitation of a nuclear spin system in crystals with a large dynamic frequency shift

V. P. Chekmarev and M. P. Petrov

A.F. Ioffe Physico-technical Institute, USSR Academy of Sciences

(Submitted February 10, 1976)

Zh. Eksp. Teor. Fiz. 71, 377-392 (July 1976)

Some features of the formation of nuclear spin echo in crystals with a large dynamic frequency shift are investigated at a strong detuning between the NMR frequency and the pulse carrier frequency (nonresonant excitation). Expressions for the intensity and time of appearance of nuclear echo under these conditions are obtained by solving the equations of motion. The dependence of the echo amplitude on the exciting-pulse duration and on the magnitude of the detuning is analyzed. The optimal conditions for observing the echo under conditions of strong detuning are determined. The nature of the shift in time of appearance of the echo is elucidated and the dependence of the shift on the detuning is determined. The influence of the approximations employed in the analysis is assessed. The theoretical results are compared with the experimental data. The conditions for observing oscillations in the nuclear echo spectrum are considered. Results are presented of an experimental investigation and numerical analysis of the oscillation depth and its dependence on the intensity of the radio-frequency pulses.

PACS numbers: 76.60.-k

INTRODUCTION

The behavior of a system of nuclear spins in magnetically-ordered crystals is determined practically completely by the hyperfine interactions.^[1] In an analysis of the NMR spectra in these crystals it is important to take into account the reaction of the nuclear moments on the electron system. This influence leads to a number of nonlinear effects, particularly to a dependence of the precession frequency ω_n of the nuclear magnetization m on the projection of the vector m on the equilibrium direction z ^[2,3]:

$$\omega_n = \omega_{n0} - \omega_p m_z / m, \quad (1)$$

where ω_{n0} is the undisplaced NMR frequency, ω_p is the dynamic frequency shift (DFS). The influence of the DFS is particularly strong in weakly anisotropic ferromagnets RbMnF_3 , CsMnF_3 , KMnF_3 , MnCO_3 , and MnO ,^[1] where the ratio $\omega_p / \omega_{n0} \sim 0.1$ even at helium temperatures. At the present time it can be regarded as proved that the nuclear spin echo in these substances is formed at $T = 1.5 - 4.2$ °K not by the Hahn phase mechanism^[4] but by a frequency modulation (FM) mechanism,^[5,6] since the Hahn mechanism is not effective under these conditions.

Investigations of the singularities of the spectrum of nuclear spin echo in crystals with large DFS, namely RbMnF_3 ,^[7] MnCO_3 and CsMnF_3 ,^[8] have shown that two echo-excitation regimes exist in these crystals:

1. At low powers of the radio-frequency (RF) pulses, the intensity of the two-pulse echo is maximal upon excitation of nuclear spins at the frequency at the center of the NMR line (i.e., in the absence of a difference between ω_{NMR} and ω_{RF} —case of resonant excitations). The echo spectrum agrees well with the stationary-NMR data, and the echo intensity decreases abruptly with increasing detuning. Similar properties are possessed by nuclear echo in ordinary crystals without DFS.^[9]

2. At high powers and at the same pulse durations, under conditions of resonant excitations, no nuclear echo is observed.^[7] The echo intensity is maximal at a certain difference between ω_{NMR} and ω_{RF} , and the echo can be observed at appreciable detunings, much larger than the width of the NMR line. (For example, in RbMnF_3 at $T = 1.5$ °K and at a line width $\sigma / 2\pi \sim 0.5$ MHz echo was observed at detunings up to $\Delta\omega_0 / 2\pi \sim 6$ MHz.) The dependence of the echo intensity on the detuning can have a complicated character (see Fig. 1 of^[7]), but the echo signal always coincides with the NMR frequency, with the exception of the special case of "capture" echo.^[8] Thus, at large radio-frequency pulse powers, a new method of exciting the system of nuclear spins in crystals with large DFS is observed, namely nonresonant excitation ($\Delta\omega_0 \gg \sigma$, but $\omega_1 \ll \Delta\omega_0$, where ω_1 is the amplitude of the RF field at the nuclei in frequency units). Understandably, the nuclear echo in nonresonant excitation is formed by the FM mechanism, since the Hahn mechanism is not effective at large detunings ($\Delta\omega_0 \gg \sigma$ and $\Delta\omega_0 \gg \omega_1$).^[9]

Under conditions of nonresonant excitation, the nuclear echo has many unique properties: an appreciable difference can occur between the time that the echo is produced and double the delay time between the pulses, a periodicity in the dependence of the echo intensity on the detuning at a constant power of the exciting pulses,^[7] a strong dependence of the echo intensity on the RF pulse duration, the existence of single-pulse and capture echo, an increase of the maximum value of the echo intensity with increasing detuning, the special role of the fronts of the exciting pulses in the formation of the single-pulse echo,^[8] etc.

However, an FM-mechanism theory that yields results convenient for comparison with experiment has been developed only for the case when there is no detuning (resonant excitation).^[5] A general expression for the intensity of two- and three-pulse echos in crystals with large DFS in the case of linear trajectories has

been obtained only in integral form,^[3] which is suitable in many cases only for asymptotic estimates. Under nonresonant-excitation conditions it was therefore possible only to estimate roughly or to interpret qualitatively many properties of nuclear echo. A generalization of the results of the theory of the FM mechanism under resonant excitation^[5] to include the case of large detunings, as proposed in^[8] (by replacing the rotation angles of the nuclear magnetization by their maximum value) is incorrect, since in the case of nonresonant excitation it is necessary to take into account the singularities of the motion of the nuclear magnetization during the time of action of the pulse.^[9,11]

We obtain in this paper an explicit expression for the intensity of the nuclear echo and for the time of its appearance under conditions of nonresonant excitation of nuclear spins. On the basis of the proposed theory we analyze the properties of the nuclear echo at large detunings between the echo frequency and the carrier frequency of the exciting RF pulses. Experimental data and the results of a numerical analysis are presented for the depth of the oscillations observed in^[6] in the nuclear-echo spectrum. These oscillations can serve as a criterion for the effectiveness of the FM mechanism of echo formation.

NUCLEAR ECHO AT NONRESONANT EXCITATION

To calculate the nuclear-echo intensity at large detunings it is necessary to take into account the peculiarities of the motion of the nuclear magnetization during the time of action of the RF pulses. To this end it is necessary in the general case to solve the system of equations of motion of nuclear isochromates in the effective field

$$\mathbf{H}_{effj} = \frac{1}{\gamma_n} (\Delta\omega_j \mathbf{z} + \omega_j \mathbf{y}). \quad (2)$$

Here γ_n is the gyromagnetic ratio, $\Delta\omega_j = \omega_j - \omega_{RF}$ is the deviation of the NMR frequency for the j -th isochromate from the RF-pulse carrier frequency, and z and y are unit vectors in a coordinate system rotating at the RF-field frequency. The equations of motion for the j -th isochromate in this rotating system (RCS)^[10] take the form

$$\begin{aligned} \frac{dX_j}{dt} &= Y_j \Delta\omega_j \left(1 + \delta Z_j \frac{\omega_{pj}}{\Delta\omega_j} \right) - \omega_j (1 - \delta Z_j), \\ \frac{dY_j}{dt} &= -X_j \Delta\omega_j \left(1 + \delta Z_j \frac{\omega_{pj}}{\Delta\omega_j} \right), \quad \frac{d\delta Z_j}{dt} = -\omega_j X_j, \end{aligned} \quad (3)$$

where $\delta Z_j = 1 - Z_j$, $X_j = m_{xj}/m_0$, $Y_j = m_{yj}/m_0$, $Z_j = m_{zj}/m_0$, m_0 is the equilibrium value of the nuclear magnetization of the isochromate, and t is the time. We assume that the pulse duration τ_p is short in comparison with the transverse relaxation time T_2 ($\tau_p \ll T_2$), so that the relaxation processes during the time of action of the pulses are disregarded. The solutions of the system (3) are in the general case very cumbersome and require numerical methods for their analysis.^[11] It turned out, however, that the FM mechanism of echo formation is effective only in the case when the influence of the change of the precession frequency (1) on the mo-

tion of the nuclear-magnetization vector during the time of action of the pulse can be neglected,^[1] i. e., in the case of the so-called linear trajectories (linearity criterion, see^[13]).

Thus, for the case of large detunings, when the trajectory linearity condition is satisfied, we can neglect the second term in the first and third equations of the system (3), i. e.,

$$\frac{\omega_{pj}}{\Delta\omega_j} \delta Z_j \ll 1. \quad (4)$$

At large detunings ($\omega_1/\Delta\omega_j \ll 1$) we can neglect also the fourth term in the first equation of the system (3) $\omega_1 \delta Z_j$. It can be shown that in our case allowance for this term leads to corrections to the expression for the amplitude of the transverse components of the nuclear magnetization, of the order of

$$(\omega_1/\Delta\omega_j)^2 \ll 1. \quad (5)$$

For the case of large detunings we obtain ultimately a simple system of equations of motion of the nuclear magnetization

$$\begin{aligned} \frac{dX_j}{dt} &= Y_j \Delta\omega_j - \omega_j, \quad \frac{dY_j}{dt} = -X_j \Delta\omega_j, \\ \frac{d\delta Z_j}{dt} &= -\omega_j X_j. \end{aligned} \quad (6)$$

Solving it at zero initial conditions, we obtain at the instant when the first RF pulse is turned off ($t = \tau_1$)

$$\begin{aligned} X_j &= -\frac{\omega_1}{\Delta\omega_j} \sin \Delta\omega_j \tau_1, \quad Y_j = -\frac{\omega_1}{\Delta\omega_j} \cos \Delta\omega_j \tau_1 + \frac{\omega_j}{\Delta\omega_j}, \\ \delta Z_j &= (\omega_1/\Delta\omega_j)^2 (1 - \cos \Delta\omega_j \tau_1), \end{aligned} \quad (7)$$

where τ_1 is the duration of the second pulse and $\omega_1/\Delta\omega_j \ll 1$. Let us calculate the shift of the precession frequency of the j -th isochromate $\Delta\omega_{pj1}^{\parallel}$, due to the action of the first pulse. Since the precession frequency depends on m_z [Eq. (1)] we have

$$\Delta\omega_{pj1}^{\parallel} = \omega_{pj} \delta Z_j = \omega_{pj} (\omega_1/\Delta\omega_j)^2 (1 - \cos \Delta\omega_j \tau_1). \quad (8)$$

Thus, the detuning $\Delta\omega_{1j}$ for the j -th isochromate following the application of the first pulse is

$$\Delta\omega_{1j} = \Delta\omega_j + \Delta\omega_{pj1}^{\parallel}. \quad (9)$$

In the interval between the pulses, the motion of the transverse components (in the same RCS as before) is described by the equations

$$\begin{aligned} X_j &= \frac{\omega_1}{\Delta\omega_j} [-\sin(\Delta\omega_j \tau_1 + \Delta\omega_{1j} t_1) + \sin \Delta\omega_{1j} t_1] \exp\left\{-\frac{t_1}{T_2}\right\}, \\ Y_j &= \frac{\omega_1}{\Delta\omega_j} [-\cos(\Delta\omega_j \tau_1 + \Delta\omega_{1j} t_1) + \cos \Delta\omega_{1j} t_1] \exp\left\{-\frac{t_1}{T_2}\right\}. \end{aligned} \quad (10)$$

The time t_1 is reckoned in (10) from the end of the first pulse. We express (8) and (10) in a more illustrative form:

$$\begin{aligned} X_j &= -\alpha \lambda_{1j} \cos(1/2 \Delta\omega_j \tau_1 + \Delta\omega_{1j} t_1) \exp\{-t_1/T_2\}, \\ Y_j &= \alpha \lambda_{1j} \sin(1/2 \Delta\omega_j \tau_1 + \Delta\omega_{1j} t_1) \exp\{-t_1/T_2\}, \\ \Delta\omega_{pj1}^{\parallel} &= 1/2 \omega_{pj} \alpha^2 \lambda_{1j}^2, \end{aligned} \quad (11)$$

where

$$\alpha = \omega_1 \tau_1, \quad \lambda_{1j} = \sin^{1/2} \Delta \omega_j \tau_1 / \Delta \omega_j \tau_1. \quad (12)$$

Expressions (11) differ from the corresponding expressions for the case of resonant excitation (see Eq. (7) of [5]) in the presence of a modulating factor λ_{1j} and of a corresponding phase increment. Solving the system (6) with initial conditions (11) (at $t_1 = \tau_{12}$, where τ_{12} is the delay between the pulses), we obtain for the transverse components, after the action of the second RF pulse of duration τ_2

$$\begin{aligned} X_j &= -\alpha \lambda_{1j} \cos[\Delta \omega_j (\tau_1/2 + \tau_2) + \Delta \omega_{1j} \tau_{12} + \Delta \omega_{2j} t_2] \\ &\times \exp\{-(\tau_{12} + t_2)/T_2\} - \beta \lambda_{2j} \cos^{1/2} \Delta \omega_j \tau_2 + \Delta \omega_{2j} t_2 \\ &\quad \times \exp\{-t_2/T_2\}, \\ Y_j &= \alpha \lambda_{1j} \sin[\Delta \omega_j (\tau_1/2 + \tau_2) + \Delta \omega_{1j} \tau_{12} + \Delta \omega_{2j} t_2] \\ &\times \exp\{-(\tau_{12} + t_2)/T_2\} + \beta \lambda_{2j} \sin^{1/2} \Delta \omega_j \tau_2 + \Delta \omega_{2j} t_2 \exp\{-t_2/T_2\}, \end{aligned} \quad (13)$$

where

$$\begin{aligned} \beta &= \omega_1 \tau_2, \quad \lambda_{2j} = \frac{\sin^{1/2} \Delta \omega_j \tau_2}{\Delta \omega_j \tau_2}, \\ \Delta \omega_{2j} &= \Delta \omega_{1j} + \Delta \omega_{p2}^{\parallel} + \Delta \omega_{p2}^{\perp} \cos \left[\Delta \omega_j \left(\frac{\tau_1 + \tau_2}{2} \right) + \Delta \omega_{1j} \tau_{12} \right], \\ \Delta \omega_{p2}^{\parallel} &= \Delta \omega_{p2} \beta^2 \lambda_{2j}^2, \quad \Delta \omega_{p2}^{\perp} = \omega_{p2} \alpha \beta \lambda_{1j} \lambda_{2j} \exp\{-\tau_{12}/T_2\}, \end{aligned} \quad (14)$$

$\Delta \omega_{2j}$ is the detuning for the j -th isochromate after the action of the second pulse, $\Delta \omega_{p2}^{\parallel}$ is the shift of the precession frequency of the j -th isochromate and is due to the deflection of its Z component under the influence of the second pulse, $\Delta \omega_{p2}^{\perp}$ is the amplitude of the frequency shift due to the appearance of the Z component when the transverse components of the j -th isochromate are deviated, and t_2 is the running time now reckoned from the end of the second pulse.

We have neglected in (13) and (14) the difference between $\Delta \omega_j$ and $\Delta \omega_{2j}$ during the time of action of the first and second pulses, inasmuch as in the case of linear trajectories, when a two-pulse echo is observed, there is satisfied the condition that the change in phase due to the precession frequency shifts during the time of action of the pulses be small [3]

$$\Delta \omega_{pk}^{\parallel(\perp)} \tau_k \ll 1, \quad k=1, 2. \quad (15)$$

The total shift of the isochromate precession frequency by the second pulse (14) depends on the phase of its perpendicular component towards the end of the second pulse, and is indeed the cause of the phasing of the transverse components of the isochromates in the FM mechanism of echo formation. We note that (14) coincides with the corresponding expressions (18)–(20) of the paper of Turov and Kurkin, [3] obtained with the aid of the Cayley-Klein parameters. Assuming, just as in [5], that the width of the NMR line in the considered crystals is determined by the scatter of the dynamic frequency shift ω_{pj} , [2] we separate the inhomogeneous parts of ω_{pj} and of the detuning:

$$\Delta \omega_j = \Delta \omega_0 + \Omega_j, \quad \omega_{pj} = \omega_{p0} - \Omega_j, \quad (16)$$

where $\Delta \omega_0$ and ω_{p0} are the detuning and the dynamic

shift for the center of the NMR line, and $\Omega_j = \omega_j - \omega_0$ is the difference between the frequencies of the j -th isochromate and of the line center. The signs in (16) were chosen in accordance with the definitions of the detuning and of the dynamic shift ($\Delta \omega_j = \omega_j - \omega_{RF}$; $\omega_{pj} = \omega_{p0} - \omega_j$). For crystals with large DFS we have $\omega_{p0} \gg \sigma$, and for the considered case of large detunings $\Delta \omega_0 \gg \sigma$ (σ is the line width). We can thus assume that

$$\omega_{p0} \gg |\Omega_j|, \quad |\Delta \omega_j| \gg |\Omega_j|. \quad (17)$$

To determine the echo-signal intensity it is necessary to integrate (13) over the line width, i. e., over Ω_j . We shall consider below the dependence of the various parameters in (13) on Ω_j .

1. The parameters λ_j are slowly varying functions of Ω_j (12), (14), (16) in comparison with $\Delta \omega_{2j}$ (14), since $\tau_k \ll \tau_{12}$ ($k=1, 2$). We therefore neglect the inhomogeneity of λ_j over the line in the amplitudes X_j and Y_j (13).³⁾

2. The frequency shift $\Delta \omega_{p2}^{\perp}$ (14), due to the action of the second pulse on the perpendicular components of the nuclear magnetization, will enter in the final result into the argument of the Bessel functions $p = \Delta \omega_{p2}^{\perp} t'$ (t' is the time of appearance of the echo). Consider the case $p \leq 1$; then the parameter p is a slowly varying function of Ω_j within the limits of the line width, and the inhomogeneity of $\Delta \omega_{p2}^{\perp}$ can be neglected. The condition $p \leq 1$ is well satisfied under the experimental conditions (see [7]) at $\tau_{12} \gg T_2$, since $\Delta \omega_{p2}^{\perp} \propto \exp\{-\tau_{12}/T_2\}$ (14).

3. We take the inhomogeneity of $\Delta \omega_{p2}^{\parallel}$ and $\Delta \omega_{p2}^{\perp}$ (11), (14) into account in the linear approximation, recalling that λ_j (12), (14) and ω_{pj} (16), (17) are slowly varying functions of Ω_j within the limits of the line width. For example,

$$\Delta \omega_{p2}^{\parallel}(\Omega_j) \approx \Omega_j [d\Delta \omega_{p2}^{\parallel}(\Omega_j)/d\Omega_j]_{\Omega_j=0}. \quad (18)$$

The influence of the nonlinearity of $\Delta \omega_{p2}^{\parallel}$ will be taken into account later on.

With allowance for the approximations made, assuming a Gaussian line shape as in [5], and employing the standard procedure for calculating the echo-signal intensity for the case of the FM mechanism, [13] by using the tabulated integrals [14] and the expansion

$$\exp\{iz \cos \varphi\} = \sum_{k=-\infty}^{\infty} J_k(z) \exp\{ik\varphi\}, \quad (19)$$

$$\frac{1}{\sigma \sqrt{2\pi}} \int_{-\infty}^{\infty} \exp\left\{-\frac{x^2}{2\sigma^2} \pm ipx\right\} dx = \exp\left\{-\frac{1}{2} p^2 \sigma^2\right\},$$

we obtain for the intensity amplitude of the primary echo in the case of nonresonant excitation

$$I_1 = c \eta m_0 [\alpha^2 \lambda_{1j}^2 J_1^2(p_1) \exp\{-2\tau_{12}/T_2\} + \beta^2 \lambda_{2j}^2 J_1^2(p_1)]^n \exp\{-t'/T_2\}, \quad (20)$$

where $J_1(p_1)$ and $J_2(p_1)$ are Bessel functions of the argument p_1 ,

$$p_1 = \omega_{p0} \alpha \beta \lambda_{1j} \lambda_{2j} \exp\{-\tau_{12}/T_2\}, \quad (21)$$

$$\lambda_k = \sin^{1/2} \Delta \omega_k \tau_k / \Delta \omega_k \tau_k, \quad k=1, 2,$$

c is a coefficient that reflects the geometry of the experiment (the filling factor, the properties of the resonant system, and the attenuation produced by the matching elements), η is the gain of the RF field, t' is the time of appearance of the signal and primary echo, reckoned from the end of the second pulse:

$$t' = \frac{\tau_{12} + 1/2(\tau_1 + \tau_2)}{1 + (d\Delta\omega_{p2}^0(\Omega_j)/d\Omega_j)_{\Omega_j=0}} = \frac{\tau_{12} + 1/2(\tau_1 + \tau_2)}{1 + (\omega_1\tau_2)^2(\omega_{p0}\tau_2)S}, \quad (22)$$

$$S = \frac{1}{\Delta\omega_0\tau_2} \left[\frac{\sin \Delta\omega_0\tau_2}{\Delta\omega_0\tau_2} - \left(\frac{\sin 1/2\Delta\omega_0\tau_2}{1/2\Delta\omega_0\tau_2} \right)^2 \right].$$

In the derivation of (22) we used the fact that in the considered class of crystals with large DFS, the condition $\omega_{p0}\tau_2 \gg 1$ is always satisfied at the experimentally employed pulse durations $\tau_2 \sim 1 \mu\text{sec}$. Expression (20) shows that within the framework of these approximations a nuclear echo is formed at large detunings only by the frequency-modulation mechanism ($I_1 = 0$ at $\omega_{p0} = 0$). Allowance for the term $\omega_1 \delta Z_j$ in the first equation of the system (3) yields the Hahn contribution to the echo intensity, but the magnitude of this contribution is small in comparison with (20) and will therefore be neglected in the subsequent analysis.

For the secondary echo signals, the results of the integration is analogous to (20). For example, the expression for the intensity of the n -th secondary echo is

$$I_n = c\eta m_0 [\alpha^2 \lambda_1^2 J_{n+1}(p_n) \exp\{-2\tau_{12}/T_2\} + \beta^2 \lambda_2^2 J_n^2(p_n)]^{1/2} \exp\{-n\tau'/T_2\},$$

$$p_n = n p_1 = \omega_{p0} \alpha \beta \lambda_1 \lambda_2 n \tau' \exp\{-\tau_{12}/T_2\}. \quad (23)$$

Comparing the amplitudes of the primary echo for the resonant Eq. ((13) of [5]) and nonresonant (20) excitations, we see that the corresponding expressions have different coefficients λ_k (21) in the echo amplitude and in the argument of the Bessel functions. These expressions coincide for the case of very short pulses (i.e., at $\Delta\omega_0\tau_k \ll 1$). The indicated limiting transition is valid also for secondary echo signals. We note that since the same mechanism forms the nuclear echo in the case of resonant and nonresonant excitations, the nuclear-echo spectrum should exhibit oscillations also in the considered case of large detunings [6] (for a suitable choice of the line width and receiver band width).

TIME OF APPEARANCE OF NUCLEAR-ECHO SIGNAL AT NONRESONANT EXCITATION

In crystals without DFS (the Hahn mechanism) the nuclear-echo signal appears at a time τ_{12} after the end of the second pulse. An experimental investigation of the properties of the nuclear echo in crystals with large DFS has shown that in this case the time of appearance of the nuclear echo depends on the experimental conditions—on the duration of the exciting pulses, on the employed detuning, on the pulse power, etc. The difference between the time of echo appearance and τ_{12} in crystals with large DFS, in the case of nonresonant excitation (22), has a simple and lucid interpretation from the point of view of formation of echo signals by the FM mechanism as a result of beats between equidistant oscillators. [6, 15] This interpretation makes it also possible to take into account the influence of the approximations made in the derivation of (22).

The change of the isochromate precession frequency, due to the action of the second pulse $\Delta\omega_{p2}$, consists of two terms:

$$\Delta\omega_{p2} = \Delta\omega_{p2}^0 + \Delta\omega_{p2}^1 \cos \Delta\omega_j [\tau_{12} + 1/2(\tau_1 + \tau_2)], \quad (24)$$

where $\Delta\omega_{p2}^0$ and $\Delta\omega_{p2}^1$ are defined in (14). We consider the realistic case $\tau_{12} \gg \tau$ and $\tau_{12} \gg \tau_2$, and also

$$2\pi/\tau_{12} \ll \sigma < 2\pi/\tau_2. \quad (25)$$

For example, for RbMnF_3 [7] at $\tau_2 = 1 \mu\text{sec}$, $\tau_{12} = 25 \mu\text{sec}$, and $\sigma/2\pi = 0.3 \text{ MHz}$, the inequality (25) is sufficiently well satisfied. Both terms in (24) are oscillating functions of Ω_j , but the oscillation period of the first term is $\sim 1/\tau_2$ and that of the second $\sim 1/\tau_{12}$ (since $\tau_{12} \gg \tau_2$). Taking (25) into account, we see that the first term is a slowly varying function within the limits of the line width, while the second is a rapidly varying function.

The second term in (24) describes isochromate precession-frequency variations that are periodic in Ω_j and lead to a periodic redistribution of the isochromate density over the line. As a result of the described change in the shape of the NMR line, frequency clusters of isochromates separated by an interval $\Delta\omega$ are produced [6, 15] (Fig. 1):

$$\Delta\omega = \frac{2\pi}{\tau_{12} + 1/2(\tau_1 + \tau_2)} \approx \frac{2\pi}{\tau_{12}}.$$

If the first term were homogeneous, it is these isochromate clusters which would give the echo signals at instants of time approximately equal to $k\tau_{12}$ ($k = 1, 2, \dots$). The first term in (24), $\Delta\omega_{p2}^0$, which is a slowly varying function of Ω_j within the limits of the line width, deforms the NMR line by changing the distance between the frequency clusters (see Fig. 2). By way of example, at the detuning shown in Fig. 2(a), the isochromates with the lower frequency obtain a larger frequency increment (described by $\Delta\omega_{p2}^1$). The NMR becomes narrower, and this leads to a decrease of the distance between the frequency clusters formed by the second term in (24), and to an increase in the distance between the

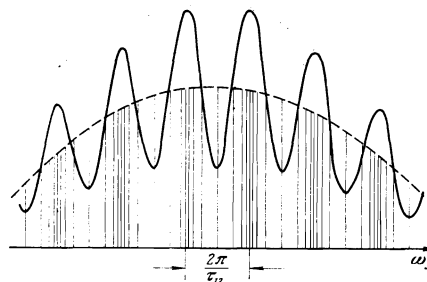


FIG. 1. Schematic representation of the change of the NMR line shape under the influence of the second pulse. Dashed—initial line shape: The vertical lines show the change in the density of the isochromates with frequency, which leads to the oscillating shape of the line. The interval between the clusters is $\Delta\omega \approx 2\pi/\tau_{12}$, where τ_{12} is the delay between the pulses.

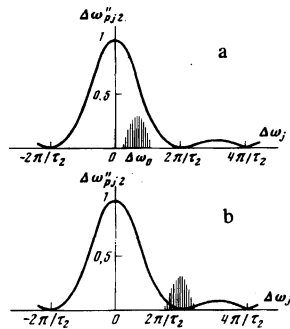


FIG. 2. Illustration of the influence of the first term $\Delta\omega_{p/2}^{II}$ in (24) on the time of the appearance of the echo signal, see (14)

$$\frac{\Delta\omega_{p/2}^{II}}{\Omega} = \left(\frac{\sin^{1/2}\Delta\omega_1\tau_2}{1/2\Delta\omega_1\tau_2} \right)^2, \quad \Omega = \frac{1}{2}\omega_p\beta^2.$$

The NMR line is shown in the form of a set of clusters representing the second terms of (24), a—at the indicated value of the detuning $\Delta\omega_0$ the NMR line becomes narrower ($t' > \tau_{12} + \frac{1}{2}(\tau_1 + \tau_2)$); b—at $\Delta\omega_0 = 2\pi/\tau_2$ the left half of the line becomes narrower and the right half broadens, leading to a doubling of the echo signal. τ_2 is the duration of the second pulse.

echo signal and the second pulse ($t' > \tau_{12}$). It is easy to calculate the distance, in frequency units, between the clusters when account is taken of the inhomogeneity of the first term $\Delta\omega_{p/2}^{II}$ in (24) (Fig. 2a):

$$\Delta\omega' = \frac{2\pi}{\tau_{12}} + \frac{2\pi}{\tau_{12}} \left[\frac{d\Delta\omega_{p/2}^{II}(\Omega_j)}{d\Omega_j} \right]_{\Omega_j=0},$$

giving echo signals at instants of time that are multiples of t' :

$$t' = \frac{2\pi}{\Delta\omega'} = \frac{\tau_{12}}{1 + (d\Delta\omega_{p/2}^{II}(\Omega_j)/d\Omega_j)_{\Omega_j=0}}. \quad (26)$$

Expression (26), taking into account that $\tau_{12} \gg \tau_1$ and $\tau_{12} \gg \tau_2$, coincides with the result (22) obtained by integrating the equations of motion (13). The illustrative interpretation presented, however, yields additional information.

1. The nonlinearity of $\Delta\omega_{p/2}^{II}$ within the line width

$$[d^2\Delta\omega_{p/2}^{II}(\Omega_j)/d\Omega_j^2] \neq 0$$

leads to inhomogeneity of the distance between the frequency clusters (see Fig. 2), i.e., to a broadening of the echo signal and to a decrease of its intensity. Thus, the range of observation of the nonresonant excitation is limited by the inequalities (25).

2. Allowance for the inhomogeneity of the amplitude of the frequency modulation $\Delta\omega_{p/2}^I$ in (24) at $p \ll 1$ leads only to a difference in the quality of the formation of the clusters in different sections of the NMR line, but does not change the frequency distance between the clusters, i.e., in our approximation it exerts no influence on the time at which the echo signal is produced.

3. If a zero of the function $\Delta\omega_{p/2}^{II}$ falls within the limits of the line width (see Fig. 2b), i.e., if for some value of k we have

$$\Delta\omega_0 - \sigma/2 < k2\pi/\tau_2 < \Delta\omega_0 + \sigma/2, \quad k = \pm 1, \pm 2, \quad (27)$$

then the distances between the clusters on opposite sides of the considered zero of the function $\Delta\omega_{p/2}^{II}$ are different, and this leads to a splitting of the echo signal on the oscilloscope screen. This effect was observed experimentally for RbMnF_3 .

We consider now the dependence of the instant of the appearance of the echo on the detuning $\Delta\omega_0$. Expression (22) shows that in the case of nonresonant excitation t' does not depend on the detuning. Moreover, there exists a constant shift (on the order of the pulse duration) which does not depend on the detuning. Figure 3 shows the dependence of t' on $\Delta\omega_0$, calculated from formulas (22), and the results of an experimental investigation of the instant of the appearance of the echo in RbMnF_3 . At $\omega_1/2\pi = 6.5$ kHz, the agreement between the theoretical and experimental results is good. The error in the determination of constant shift lies within the experimental error. The even-in-the-detuning approach of the signal echo to the RF pulses in the case of resonant excitation (see [7], Fig. 1(a)) can be attributed to the broadening of the line as a result of the appearance of nonlinearities. [3,8,11] For this reason, the estimates made in [7] are not valid for the case of small detunings.

DEPENDENCE OF THE ECHO INTENSITY ON THE DURATION OF THE EXCITING PULSE AND ON THE DETUNING

The expression (20) for the intensity of a two-pulse echo in nonresonant excitation shows that the echo amplitude depends strongly on the duration of the exciting pulses. When the detuning is increased, the dependence becomes continuously sharper. For example, at $p \ll 1$ we have

$$I_1 \propto \sin^2 1/2\Delta\omega_0\tau_2 \sin 1/2\Delta\omega_0\tau_1. \quad (28)$$

The optimal values for the pulse durations in the case of nonresonant excitations depend on the employed detuning $\Delta\omega_0$:

$$\tau_{1 \text{ opt}} = \tau_{2 \text{ opt}} = (\pi/2 + k\pi) 2/\Delta\omega_0, \quad k=0, 1, 2, \dots, \quad (29)$$

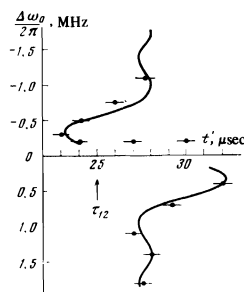


FIG. 3. Dependence of the echo-appearance time t' on the detuning $\Delta\omega_0$ between the echo frequency and the RF frequency of the pulses. Experiments on RbMnF_3 at $T = 1.5$ °K, $\tau_{12} = 25$ μsec, $\omega_p/2\pi = 45$ MHz, $\omega_1 = 2.6$ in relative units (cf. [7]), $\tau_2 = 25$ μsec, (1.0 μsec at the 0.7 level). Theoretical curve—calculation by formulas (22) at $\tau_2 = 1.3$ μsec, the constant shift is taken to be 2.7 μsec, and the adjustment parameter is $\omega_1/2\pi = 6.5$ kHz.

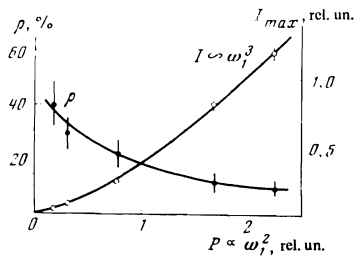


FIG. 4. Dependence of the depth of the oscillations ρ (34) and of the echo intensity I_{max} on the RF pulse power P for the central frequency of the spin-echo spectrum in RbMnF_3 at $\tau_{12} = 8 \mu\text{sec}$, $T = 1.5^\circ\text{K}$, $\tau_1 = \tau_2 = 1 \mu\text{sec}$, $H_0 = 8.8 \text{ kOe}$, and $f_{\text{NMR}} = 649 \text{ MHz}$.

i. e., the first optimum at $k=0$ is

$$\tau_1 = \tau_2 = \pi / \Delta\omega_0. \quad (30)$$

Actually, when a two-pulse echo is observed in RbMnF_3 ^[7] at large detunings, the echo signal is maximal for pulses of equal duration, and with increasing detuning the intensity of the echo increases as the duration of the employed pulses decreases. Their magnitude agreed approximately with (30). It should be noted that when the echo was observed in the absence of detuning, the echo signal was also maximal at equal pulse durations, something that does not follow from the theory of echo formation under resonant excitation.^[5] The point is that when the echo is observed in the absence of detuning it is necessary to employ RF pulses of low power ($\omega_1 \ll 1/\omega_{p0} \tau_p^2$).^[3] For the experimentally employed pulse durations $\tau_p \sim 1 \mu\text{sec}$, the condition of large detunings ($\Delta\omega_j \gg \omega_{pj}^{1/3} \omega_1^{2/3}$) is satisfied even at resonant excitation for nuclei at the edges of the NMR line, and formula (20) is then valid.

Expression (20) predicts an oscillatory dependence of the echo intensity on the detuning. For example, at $\rho \ll 1$ and at pulses of equal duration $\tau_1 = \tau_2 = \tau_p$, we have

$$I_1 \propto (\sin^{1/2} \Delta\omega_0 \tau_p^{1/2} \Delta\omega_0 \tau_p)^2. \quad (31)$$

The distance between the echo-intensity maxima is

$$\Delta\omega_n = 2\pi / \tau_p. \quad (32)$$

Oscillations of the echo intensity with changing detuning, with a period $\Delta\omega_M = 2\pi / \tau_p$, were observed experimentally in RbMnF_3 ,^[7] MnCO_3 and CsMnF_3 (private communication from Yu. M. Bun'kov), but were never explained before.

The presence of the factors λ_k (21) in (20) greatly decreases the echo intensity with increasing detuning at a constant power of the exciting pulses. Therefore observation of nuclear echo at large detunings is possible only at RF pulse powers greatly exceeding those for the case of resonant excitation (since by increasing ω_1 it is possible to compensate for the decrease of λ_k as the detuning increases). It is this which explains the main experimentally-observed difference between the two regimes of observation of nuclear echo in crystals with

large DFS.^[7,8] The maximum detuning at which nuclear echo can be observed in these crystals is determined by the limiting power of the employed RF pulse generator. The maximal echo intensity will even increase with increasing detuning, since the criterion $\Delta\omega_0 \gg \omega_{p0}^{1/3} \omega_1^{2/3}$ ^[3] for the linearity of the trajectories at large detunings makes it possible to use even larger exciting-pulse powers when the detuning is increased. This phenomenon was also observed in experiment.^[8]

OSCILLATIONS OF NUCLEAR-ECHO SPECTRUM IN CRYSTALS WITH LARGE DFS

In the investigation of the properties of nuclear-spin echo of Mn^{55} in a crystal with a large dynamic frequency shift (RbMnF_3), oscillations were observed in the nuclear-echo spectrum.^[6] When the receiver frequency was varied, the echo-signal intensity varied periodically on the oscilloscope screen (see Fig. 1 of^[6]), and the frequency of the RF pulses as well as the other experimental conditions (the external magnetic field, the pulse durations, the pulse power, the delay between pulses, etc.) were maintained constant. The average period of the oscillations in frequency units Δf_{av} , measured by counting the number of maxima as the receiver was tuned, turned out to be

$$\Delta f_{cr} = 1/\tau_{12}. \quad (33)$$

The intensities of the secondary echo signals and of the free induction after the second pulse oscillate in synchronism with the primary echo signal, as does the stimulated-echo intensity. No changes were observed in the free-induction signal intensity after the first pulse.

Our subsequent experimental investigations have shown that the depth ρ of the observed oscillations decreases with increasing RF pulse power (Fig. 4). The depth of the oscillations is defined as the ratio of the oscillation amplitude to the maximum echo-signal intensity, i. e.,

$$\rho = (I_{max} - I_{min}) / I_{max}. \quad (34)$$

It was established in addition that the depth of the oscillations of the stimulated-echo signal intensity is always larger than that of the two-pulse echo signal and that at small RF pulse powers it reaches almost 100%. The experimental conditions are described in^[6].

The possibility of observing oscillations in the nuclear-echo spectrum is due to the finite band width ΔF of the receiver for the amplified frequencies. In this case it is easy to create a situation wherein only a fraction of the nuclear-echo spectrum falls in the band width ΔF of the receiver. Then, if the echo spectrum has a fine structure, the latter is revealed by the change of the echo-signal intensity on the oscilloscope screen when the receiver frequency is tuned. It is necessary for this purpose that the condition $\Delta\Omega < a_i$ be satisfied, where $\Delta\Omega$ is the slope of the receiver bandwidth and a_i are the characteristic parameters of the fine structure, $i=1, 2, 3, \dots$. If the distances between the neighboring

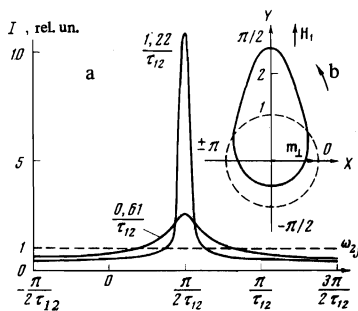


FIG. 5. a) Results of numerical calculation of the change of the line shape in the interval (36) under the influence of the second pulse for two values of the parameter $\Delta\omega_{p2\perp}$: $0.61 \tau_{12}^{-1}$ and $1.22 \tau_{12}^{-1}$. The unperturbed intensity of the line is assumed to be equal to unity. b) Phase diagram of the considered section of the line (36) at the instant when the echo is produced at $\Delta\omega_{p2\perp} = 0.61 \tau_{12}^{-1}$ in a coordinate system rotating with the frequency of the RF field. The arrows show the direction of the RF field H_1 and the direction of rotation of the isochromates with $\omega_{2j} > 0$, while m_1 is the direction of the nuclear magnetization at the instant of the termination of the second pulse; the dashed line shows the dephasing of m_1 of the considered section in the case when there is no DFS (unit circle).

singularities in the echo spectrum do not satisfy this inequality, then these singularities will not be resolved. At $\Delta F \leq \sigma_{\text{exc}}$ (σ_{exc} is the width of the excited part of the NMR line, which makes the main contribution to the echo-signal intensity), a fine structure of this echo spectrum will be registered in the entire tuning range of the receiver so long as this echo signal is reserved, but if $\Delta F > \sigma_{\text{exc}}$ it will be registered only when the slopes of the receiver bandwidth pass over the excited part of the NMR line σ_{exc} .

In the general case, the character of the fine structure of the echo spectrum can be different. First, it can be due to singularities of the investigated NMR line caused by the quadrupole splitting or by the distribution of the local fields at the investigated nuclei. In this case, if irregularities are observed in the dependence of the echo intensity of the receiver tuning frequency, the distance between them does not depend on the parameters of the exciting RF pulses. These irregularities can take the form of nonmonotonocities in the rise or fall of the echo intensity as a function of the receiver tuning frequency, and also of the oscillations. Second, the fine structure of the echo spectrum can be due to deformation of the NMR line under the influence of the RF pulses. In this case the distance between the irregularities should depend on the parameters of the employed RF pulses.

In the investigated crystals with large DFS, the second pulse alters significantly the shape of the NMR line, forming frequency clusters of isochromates that are separated by a distance $\Delta f = 1/\tau_{12}$, see Fig. 1.^[6,13,15] This leads to a fine structure of the nuclear-echo spectrum, so that the nature of the oscillations in the spin-echo spectrum of the Mn^{55} nuclei in RbMnF_3 ^[6] is qualitatively understood. However, quantitative estimates of the depth ρ of the oscillations and of its dependence on the power of the exciting RF pulses (Fig. 4) are difficult.

The point is that in the calculation of the echo-signal intensities, both in the case of resonant^[5] and nonresonant excitations (19) and (20), the equations of motion of the nuclear magnetization of the isochromates were integrated between infinite limits. Therefore the expressions obtained for the intensities of the echo signals correspond to the case $\Delta F \gg \sigma_{\text{exc}}$, i. e., when the entire spin-echo spectrum is inside the receiver band width. Understandably, these expressions describe neither the presence of oscillations in the spin-echo spectrum^[6] nor their depth.

To explain the experimental results we have integrated numerically the equations of motion of the nuclear magnetization of the isochromates between the limits $f_0 - \Delta F/2$ and $f_0 + \Delta F/2$, where f_0 is the average frequency to which the receiver is tuned, and varies in the course of tuning. In the integration we used the limitations $\Delta F < \sigma_{\text{exc}}$, $\tau_{12} \geq T_2$ and $\Delta\omega_{p2\perp} \tau_{12} \lesssim 1$, corresponding to the real experimental conditions in RbMnF_3 .^[6] For a qualitative understanding of the results, the integration was carried out in two stages.

1. We first calculated numerically the NMR line shape after the second pulse. The changes produced in the frequencies of the isochromates by the second pulse are periodic over the NMR line⁴⁾ (24) or (8)^[5]:

$$\omega_{2j} = \omega_{1j} + \Delta\omega_{p2\perp} \cos \omega_{1j} \tau_{12}, \quad (35)$$

where ω_{1j} and ω_{2j} are the frequencies of the j -th isochromate before and after the action of the second pulse. It suffices therefore to consider the change in the line shape on a section of width $2\pi/\tau_{12}$. Consider, for example, the NMR line section

$$-\pi/2\tau_{12} \leq \omega_{1j} \leq 3\pi/2\tau_{12}. \quad (36)$$

Figure 5a shows the results of the numerical calculation of the change in the shapes of line section (36) at two values of the parameter $\Delta\omega_{p2\perp}$ (35). The unperturbed intensity of the line is assumed to be unity. Figure 5a illustrates clearly the redistribution of the isochromate density under the influence of the second pulse, which leads to formation of clusters at the frequencies

$$\omega_{cl} = \pi/2\tau_{12} + 2\pi k/\tau_{12} \quad (k=0, \pm 1, \pm 2, \dots).$$

2. Within the framework of the limitations assumed by us, we shall consider only the phasing of the transverse components of the nuclear magnetization, which are produced by the second pulse and make the main contribution to the echo-signal intensity under these conditions. We assume that immediately after the termination of the second pulse ($t=0$) these isochromates have the same phase $\varphi_0=0$, see Fig. 5b. Then, at the instant of the appearance of the echo $t \approx \tau_{12}$ the isochromates of the considered section of the line (36) will have phases in the range $-\pi/2 \leq \varphi \leq 3\pi/2$, i. e., we have considered one circle of the fan of the dephasing isochromates. By the instant $t = \tau_{12}$, all the clusters have the same directions (their phases at $t \approx \tau_{12}$ are $\varphi_{cl} = \pi/2 \pm 2k\pi$). This leads to the appearance of a nonzero transverse nuclear magnetization m_{Σ} , i. e., an echo signal,

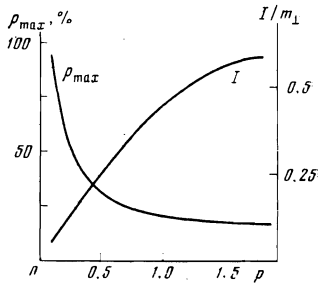


FIG. 6. Dependence of the maximum depth of oscillations ρ_{\max} and of the echo intensity on the value of the parameter $\rho = \Delta\omega_{p2} \tau_{12}$. The calculation was carried out for $\Delta F = 1$ MHz and $\tau_{12} = 7.5$ μ sec. The presented dependence was obtained by numerically integrating the contributions made to the echo signal intensity by the isochromates that fall in the receiver band as its averaged tuning frequency is changed, with allowance for the phase of the monochromates at the instant $t = \tau_{12}$. The echo intensity was obtained in units of m_1 .

in which case the isochromates with frequencies

$$0 + k \frac{2\pi}{\tau_{12}} < \omega_{2j} < \frac{\pi}{\tau_{12}} + k \frac{2\pi}{\tau_{12}} \quad (37)$$

will make a positive contribution to m_1 , while the isochromates with frequencies

$$-\frac{\pi}{\tau_{12}} + k \frac{2\pi}{\tau_{12}} < \omega_{2j} < 0 + k \frac{2\pi}{\tau_{12}} \quad (38)$$

will make a negative contribution (Fig. 5b). As the receiver is tuned, different numbers of the considered sections will fall in its bandwidth, and at $\Delta\Omega < 1/\tau_{12}$ this gives rise to oscillations of the echo intensity on the oscilloscope screen, with a period $\Delta f = \Delta\omega/2\pi = 1/\tau_{12}$. Understandably, the depth of oscillations increases with decreasing cluster intensity (with decreasing $\Delta\omega_{p2}^1$), and also with decreasing τ_{12} , which leads to a decrease of the number of clusters in the receiver band.

Analysis has shown that the depth of the oscillations of the echo intensity as the receiver is tuned depends also on the ratio of the parameters ΔF and τ_{12} , the maximum depth of oscillations being observed at a receiver bandwidth $\Delta F = (n + \frac{1}{2})/\tau_{12}$, where n is an integer. The purpose of the present calculation is to estimate the maximum depth of the oscillations at different RF pulse powers. We have therefore assumed in the calculations $\Delta F = 1$ MHz and $\tau_{12} = 7.5$ μ sec. These values satisfy the condition that ρ be maximal and are close to the experimental conditions (Fig. 4), namely $\Delta F = 1$ MHz and $\tau_{12}' = (8 \pm 0.5)$ μ sec, taking into account the real waveform of the pulses. The dependence of the depth of the oscillations and of the echo intensity on the value of the parameter $\rho = \Delta\omega_{p2}^1 \tau_{12}$, calculated at $\Delta F = 1$ MHz and $\tau_{12} = 7.5$ sec, is shown in Fig. 6. Both in the case of resonant excitation^[5] and in the case of nonresonant excitation (14) we have $\Delta\omega_{p2}^1 \propto \omega_1^2$. Thus, within the framework of our limitations, Fig. 6 shows the dependence of the maximum oscillation depth ρ_{\max} on the RF pulse power, since the parameter ρ is proportional to the power of the RF pulses P ($\rho \propto \omega_1^2 \propto P$). It is seen that with decreasing

pulse power the depth of the oscillations increases, and the intensity of the echo decreases.⁵⁾ The results of the calculations agree qualitatively with the experimental data (Fig. 4). The decrease of the depth of the oscillations at the extremal value of the receiver tuning frequency, Fig. 1,^[6] can be easily understood, for in this case only one slope of the receiver band is located on the excited part of the NMR line. The depth of the oscillations of the stimulated echo is always larger than that of the two-pulse echo, because at the same value of the pulse power we have

$$\Delta\omega_{p3}^1 \approx \Delta\omega_{p2}^1 \exp\{-\tau_{23}/T_1\}, \quad (39)$$

where τ_{23} is the delay between the second and third pulses and $\Delta\omega_{p3}^1$ is the amplitude of the frequency modulation of the NMR line at the instant $t = \tau_{23}$. With increasing τ_{23} , the depth of the oscillations of the stimulated echo will increase.

Thus, the oscillations in the nuclear-echo spectrum observed in^[8] offer clear proof that in crystals with large DFS the nuclear echo is formed by the frequency-modulation mechanism.

CONCLUSION

A study of the properties of nuclear echo in crystals with large DFS under nonresonant excitation yields more information on the subsystem of the nuclear spins and on the echo formation mechanism than the traditional method of observation: first, the very possibility of observing an intense nuclear-echo signal at large detunings between the NMR frequency and the carrier frequency of the RF pulses is a characteristic feature of systems with DFS; second, it is precisely under nonresonant excitation that many unique properties of the nuclear echo formed by the frequency-modulation mechanism appear; thirdly and finally, under these conditions it is possible to investigate in greater detail the free-induction signal as a result of pulse action on the system of nuclear spin with DFS (under nonresonant excitation the frequencies of nuclear-system response and of the pulsed action are different, so that there is no "ringing" of the receiving apparatus as a result of the action of the high-power RF pulses).

The oscillations in the nuclear-echo spectrum were observed both under resonant and nonresonant excitation, thus confirming the equivalence of the echo-formation mechanisms in both cases. This effect is one of the most pronounced features of nuclear echo in crystals with large DFS.

The authors thank A. A. Petrov for help with the experimental investigations and M. I. Kurkin and Yu. M. Bun'kov for useful discussions.

¹⁾It should be noted that while neglecting the influence of the change of the precession frequency $\Delta\omega_p$ on the motion of m during the time of action of the pulse, we must nevertheless calculate $\Delta\omega_p$ and take it into account in the interval between the pulses τ_{12} , and also between the second pulse and the echo signal, since $\tau_{12} \gg \tau_p$.

²⁾As shown in^[12], the expression for the intensity of the nuclear

echo in crystals with large DFS does not depend on any assumption concerning the nature of the inhomogeneity of the NMR line (cf. (11), (12) in^[5] and (12) in^[12]).

³) Allowance for the inhomogeneity of λ_j in the amplitudes X_j and Y_j in (13) leads to a shift of the time of the occurrence of the echo by an amount on the order of the duration of the pulses and splitting of the echo signal, which is not resolved at the actually employed $\tau_p \sim 1 \mu\text{sec}$ and an echo width 1–2 μsec .

⁴) We consider the simplest case of the homogeneity of the frequency shifts $\Delta\omega_{pj2}^{\parallel}$ and $\Delta\omega_{pj2}^{\perp}$ (the influence of the inhomogeneity is discussed in^[3,7,11]). We have also disregarded the term $\Delta\omega_{pj2}^{\parallel}$ (24), the influence of which in the inhomogeneous case reduces to the appearance of an inessential phase factor.

⁵) Figure 6 shows that at $\Delta\omega_{pj2} \perp \tau_{12} \ll 1$ the echo intensity I is proportional to ω_1^2 , since the calculation was carried out for the amplitude of the transverse components of the nuclear magnetization m_1 , which is equal to unity. Recognizing that the actual value of m_1 is proportional to ω_1 , we find that the echo intensity I is proportional to ω_1^3 , in agreement with the experimental data of Fig. 4.

¹E. A. Turov and M. P. Petrov, *Yadernyi magnitnyi rezonans v ferro- i antiferromagnetikakh* (Nuclear Magnetic Resonance in Ferro- and Antiferromagnets), Nauka, 1969.

²F. G. de Gennes, P. A. Pinkus, F. Hartman-Bourton, and M. Winter, *Phys. Rev.* **129**, 1105 (1963).

³M. I. Kurkin and E. A. Turov, *Fiz. Metal. Metalloved.* **40**, 714 (1975).

⁴E. L. Hahn, *Phys. Rev.* **80**, 580 (1950).

⁵M. P. Petrov, G. A. Smolenskii, A. A. Petrov, and S. I.

Stepanov, *Fiz. Tverd. Tela* (Leningrad) **15**, 184 (1973) [*Sov. Phys. Solid State* **15**, 126 (1973)].

⁶V. P. Chekmarev, M. P. Petrov, and A. A. Petrov, *Fiz. Tverd. Tela* (Leningrad) **17**, 1822 (1975) [*Sov. Phys. Solid State* **17**, 1193 (1975)].

⁷A. A. Petrov, M. P. Petrov, and V. P. Chekmarev, *Fiz. Tverd. Tela* (Leningrad) **17**, 2640 (1975) [*Sov. Phys. Solid State* **17**, 1755 (1975)].

⁸Yu. M. Bun'kov and B. S. Dumes, *Zh. Eksp. Teor. Fiz.* **68**, 1161 (1975) [*Sov. Phys. JETP* **41**, 576 (1975)].

⁹H. Pfeifer, *Ann. Phys. (N.Y.)* **17**, 23 (1955).

¹⁰E. A. Turov, M. I. Kurkin, and V. V. Nikolaev, *Zh. Eksp. Teor. Fiz.* **64**, 283 (1973) [*Sov. Phys. JETP* **37**, 147 (1973)].

¹¹M. I. Kurkin and V. V. Nikolaev, *Fiz. Metal. Metalloved.* **38**, 957 (1974).

¹²S. A. Zel'dovich and A. R. Kessel', *Fiz. Tverd. Tela* (Leningrad) **17**, 3137 (1975) [*Sov. Phys. Solid State* **17**, 2075 (1975)].

¹³A. A. Petrov, Author's abstract of Candidate's dissertation, Leningrad Phys. Tech. Inst., 1975.

¹⁴I. S. Gradshtein and N. M. Ryzhik, *Tablitsy integralov, summ, ryadov i proizvedenii* (Tables of Integrals, Sums, Series, and Products), Nauka, 1971 [*Academic*, 1966].

¹⁵A. S. Borovik-Romanov, Ju. M. Bunkov, B. S. Dumes, and V. A. Tulin, 18th Ampere Congress, Nottingham, 1974, Vol. 1, p. 5.

¹⁶Yu. M. Bun'kov, B. S. Dumes, and M. I. Kurkin, *Pis'ma Zh. Eksp. Teor. Fiz.* **19**, 216 (1974) [*JETP Lett.* **19**, 132 (1974)].

Translated by J. G. Adashko